

**Percentage depth dose distributions in inhomogeneous phantoms
with lung and bone equivalent media for small fields of
CyberKnife**

Chung Il Lee,¹ Jae Won Shin,² Sei-Chul Yoon,¹ Tae Suk Suh,³ Seung-Woo
Hong,^{2,4} Kyung Joo Min,⁴ Sang Deok Lee,^{2,5} Su Mi Chung,⁶ and Jae-Yong Jung⁷

¹*Department of Radiation Oncology, The Catholic University of Korea,
Bucheon St. Mary's Hospital, Bucheon, Korea*

²*Department of Physics, Sungkyunkwan University, Suwon, Korea*

³*Department of Biomedical Engineering,
the Catholic University, Seoul, Korea*

⁴*Department of Energy Science, Sungkyunkwan University, Suwon, Korea*

⁵*Department of Optometry, Gimcheon University, Gimcheon, Korea*

⁶*Department of Radiation Oncology, The Catholic University of Korea,
Yeowido St. Mary's Hospital, Seoul, Korea*

⁷*Department of Radiation Oncology,
Sanggye Paik Hospital, Inje University, Seoul, Korea*

(Dated: 31 December 2013)

Abstract

The percentage depth dose distributions in inhomogeneous phantoms with lung and bone equivalent media are studied. For lung equivalent media a Balsa wood is used, and for a soft bone equivalent media a compound material with epoxy resin, hardener and calcium carbonate is used. Polystyrene slabs put together with these materials are used as an inhomogeneous phantom. Dose measurements are performed with Gafchromic EBT film by using photon beams from 6MV CyberKnife at the Seoul Uridul Hospital. The cone sizes of the photon beams are varied from 5, 10 to 30 mm. As a simulation tool GEANT4 Monte Carlo code v9.4.p02 is used. When the Balsa wood is inserted in the phantom, the dose measured with EBT film is found to be significantly different from the dose without the EBT film in and beyond the Balsa wood region, particularly for small field sizes. On the other hand, when the soft bone equivalent material is inserted in the phantom, discrepancy between the dose measured with EBT film and the dose without EBT film can be seen only in the region of bone equivalent material. GEANT4 simulations are done with and without the EBT film to compare the simulation results with measurements. We find that the simulations including EBT film agree with the measurements for all the cases within an error of 2.2%. Also, we find the "doses to phantom" without the EBT film differ from the "doses to film" up to 29%, which shows that for accurate dose estimations for inhomogeneous phantoms with EBT film the presence of the EBT film needs to be taken into account properly in particular for small fields.

PACS numbers: 07.05.Tp, 02.70.Uu, 87.55.-x

Keywords: CyberKnife, GEANT4, Gafchromic EBT film, Inhomogeneity, Small fields

I. INTRODUCTION

Stereotactic radiosurgery (SRS) [1] uses small field sizes to deliver the maximum dose to the target and the minimum dose to its surrounding normal tissues. To facilitate the use of these small field sizes, specialized equipments such as CyberKnife [2], Gamma knife [3], multileaf collimating systems [4, 5] and etc. are needed. A higher accuracy is needed compared to conventional radiotherapy to deliver photon beams with the uncertainty of ± 1 mm at the target [6]. However, measurements of the doses for small fields, often used in SRS, are difficult due to the absence of electronic equilibrium in radiation fields of dimensions smaller than the maximum range of secondary electrons. Such difficulties associated with small beam fields bring about uncertainties in the area of clinical dosimetry.

Different dosimeters are used for small field radiations: ionization chambers, diamond detectors, silicon diodes, radiochromic films and etc. Ionization chambers have been a standard of the dose measurement and calibrations for general radiation treatment. However, ionization chambers are larger than the small beam field sizes used in SRS. Silicon diodes are often selected for stereotactic radiotherapy (SRT) and SRS because of its small sensitive volumes. However, it is energy-, dose rate- and direction-dependent [7, 8]. Silicons which have a higher atomic number than tissues are sensitive to low energy photons and thus tend to overestimate the dose at low energies. Diamond detectors which have been developed for photon dosimetry for small fields are tissue equivalent. Though its spatial resolution is good, it is very expensive and dose-rate dependent [9, 10]. Gafchromic EBT dosimetry films are near tissue-equivalent and independent of photon energy from keV to MeV ranges. Because it has a high spatial resolution and does not require film development, it is used for quality assurance of Intensity-Modulated Radiation Therapy (IMRT) and photon detection for radiosurgery of small field sizes [11, 12], though the sensitivity and accuracy of measurement could differ by the choice of densitometry system and calibration [13–16]. The EBT films, diode detectors and ion chambers produce nearly identical values of percentage depth dose (PDD) for field sizes larger than 10 mm in CyberKnife. However, for field sizes of 5 mm and 7.5 mm, these detectors do not produce identical PDDs [12]. Detailed comparisons of these detectors can be found in Table 1 of Ref. [12].

When SRS/SRT was initially implemented to the treatment of brain, inhomogeneity of the brain was not seriously considered. As the use of CyberKnife expands, however, more

accurate dose estimation is needed for tissues with inhomogeneous region, such as air cavity, lung and bones. Agreement between the treatment plan and the measured dose values for small field radiations in inhomogeneous region in spine and lung tissues is a major factor that affects treatment accuracy. Techniques to correct for inhomogeneity have been developed with increasing computing power and improved understanding of density-variable regions [17]. Accurate dose measurement is particularly important in the dosimetry of small fields in the presence of low density inhomogeneities. When the photon beams pass through the air cavity, which is the lowest density area in the human body, the dose drops in the air cavity, whereas it gets built-up in the phantom, and thus a dose enhancement may be developed in the distal side of cavity [17–20].

The characteristics of the inhomogeneous conditions were studied with the radiochromic film type MD-55 (Gafchromic type MD-55 Cat no 37-041 Lot no J1548MD55) by Paelinck *et al.* [18, 21]. They performed the dose measurement with films and Monte Carlo simulations for inhomogeneous phantoms involving the air cavity or lung equivalent media with the photon beams provided by 6MV linear accelerator. In their simulations, they modeled the phantoms and the film by using BEAMnrc/EGSnrc system and then compared the simulation results with measurements, obtaining consistency between the film measurements and the calculations with including the film. The dose calculations were performed in two different methods. First, the simulations were performed with a film detector, and thus the doses were obtained from the film. We refer to these values of dose as the "dose to film (DTF)". Second, the simulations were done with phantom geometry without including the film. In this case, the absorbed doses were calculated in the phantom material itself without taking into account the presence of the film. So, we call these values of dose the "dose to phantom (DTP)". For the case when the air cavity was inserted in the phantom, they found a difference between the DTF and the DTP [18, 21]. They showed that the differences decrease as the field size and the density of the medium increase. Also they found that these differences disappear by offsetting the film sideways by a few centimeters.

A study of PDD for inhomogeneous phantoms with a Balsa wood as a low density material or a cortical bone as a high density material was done by Wilcox and Daskalov [22], who compared the EBT film measurements of PDD (DTF) with the calculations of DTP for inhomogeneous conditions by using Cyberknife systems. In that work, they did not include the presence of the EBT film in the simulation since the film thickness was smaller than the

pixel size of the CT image. Thus they compared the calculated DTP with the measured DTF. In the region of low density materials such as a Balsa wood, calculations ignoring the film material did not make a noticeable difference. Beyond the Balsa wood region, however, the calculated DTP was found to be larger than the measured DTF [22]. Similar behavior can be observed in the works of Paelinck *et al.* [18, 21]. For inhomogeneous phantoms with high density materials, discrepancies between the DTF and the DTP were observed in the cortical bone region. The ratios of the DTF to the DTP in cortical bone regions were consistent with the correction factors suggested by Siebers *et al.* [23].

The discrepancy between the DTP and the DTF increases as the field size decreases. Thus, if the beam field size becomes smaller than previously considered [18, 21, 22], it can make more difference between the DTP and the DTF in inhomogeneous conditions. At present, 5 mm is the smallest cone size of the CyberKnife systems. Previously, due to the rare use of 5 mm cone size in clinical practice, this small cone size was not considered seriously. However, as an extension of the previous studies of the inhomogeneous conditions [18, 21, 22], we have considered in this work low and high density materials for inhomogeneous phantoms with 5, 10 and 30 mm cone sizes of the photon beams produced by 6MV CyberKnife and performed both simulations and measurements of PDD.

For the calculation of PDD, we used GEANT4 v9.4.p02 [24], which can simulate particle transport in matter and calculate the dose. Carrier *et al.* [25] validated the GEANT4 v5.2 for electron and photon transportation in homogeneous and multilayer phantoms. They showed that the doses obtained by GEANT4 results are comparable to those obtained by using other commonly used codes, such as MCNP, EGSnrc and EGS4. Poon *et al.* [26, 27] performed a test of consistency of GEANT4 v6.2.p01 against EGS4 and the existing data. Elles *et al.* [28] found that an improvement has been made in the version 8.3 of GEANT4 by employing the same conditions as used by Poon *et al.* [26, 27]. Also, we applied GEANT4 v9.1 to a ^{60}Co therapy unit and calculated PDD distributions, peak scatter factors and tissue air ratios [29]. We obtained consistency between the calculations and the published data (BJR suppl.25) [30] with errors less than 1%. In addition, we have simulated photon beams produced by 6MV CyberKnife system at the Seoul Uridul Hospital with GEANT4 v9.2.p01 [31], where we found that the calculated values of PDD distributions, output factors and off axis ratios agree well with the experimental values measured with silicon diode detectors within 2% errors.

In this work, we consider an inhomogeneous phantom with spine or lung equivalent materials and compare the calculated absorbed doses with the measured ones. Measurements have been done with Gafchromic EBT2 films. To see the effect of the presence of the EBT2 film on the PDD, we have performed the simulations with and without the EBT2 films. Also, we compared the measured values of PDD with the calculated values using Multiplan which is the software program used in CyberKnife treatment systems.

II. METHODS

A. Experiment

Figure 1 shows a schematic diagram and a photo of the phantom used in this work. In Fig. 1 (a), the horizontal slab of 3 cm thickness inserted in the phantom denotes the part for lung or bone equivalent materials. Gafchromic EBT2 film is inserted vertically in the middle of the phantom. The phantom is composed of polystyrene material except for the inhomogeneous region. The size of the phantom is 15 cm in width and 7.5 cm in lateral length. The total depth of the phantom is 15 cm, which consists of 3 cm of polystyrene, 3 cm of Balsa wood or soft bone equivalent material and 9 cm of polystyrene. Polystyrene is used for the soft tissue. Balsa wood and soft bone equivalent materials are used to simulate low-density medium and high-density medium, respectively. The cross section of Balsa wood has many microscopic holes and is similar to the lung. We have used the Balsa wood with density of 0.116 g/cm^3 . This value of density is about 50% lower than the one used in Ref. [22]. This choice is good to observe the difference between the DTP and the DTF. For high density materials, we have used soft bone equivalent materials. According to White *et al.* [32] the average density of the spine is 1.320 g/cm^3 . We made a soft bone equivalent material comprised of epoxy resin (40%), hardener (20%) and calcium carbonate (40%). Compounds of epoxy resin and calcium carbonate can be appropriate materials to substitute for spinal tissues because their compositions are similar to each other. Such soft bone equivalent materials used in our study have a density of 1.363 g/cm^3 .

The EBT2 film was wedged tightly in the middle of the phantom to minimize dose perturbation. Then the phantom with the EBT2 film was irradiated by photon beams with 5, 10 and 30 mm cone sizes. The source to surface distance (SSD) was chosen as 80 cm, and

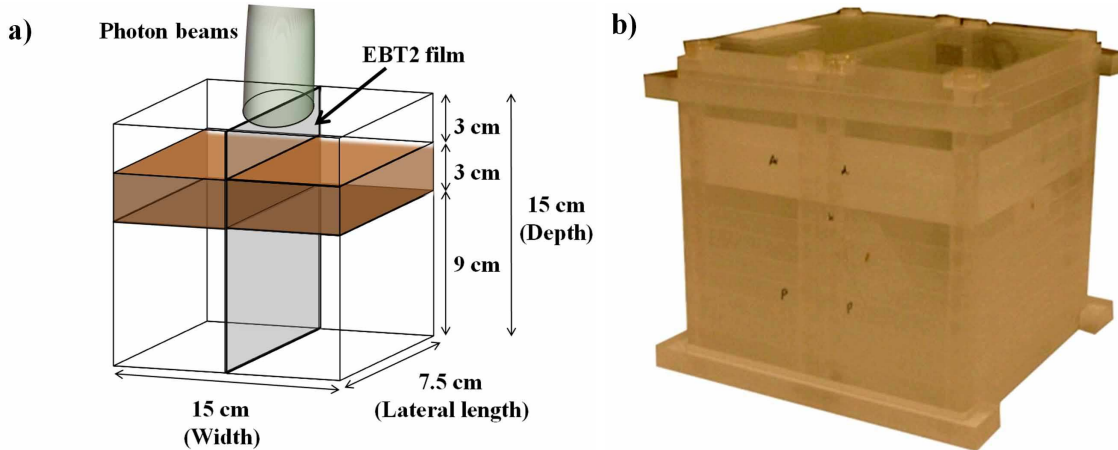


FIG. 1: (Color online) The inhomogeneous phantom has a dark horizontal part which represents either the Balsa wood or bone equivalent materials. Photon beams are irradiated from the top in parallel to the film which is inserted vertically in the middle of the phantom. A photo of the phantom is shown in (b).

irradiation dose was set to 400 cGy at the maximum dose position. Gafchromic EBT2 films were calibrated and scanned after 24 hours by the scanner Epson V700 PHOTO (Epson USA). The optical density was analyzed with OmniPro-IMRT. The CyberKnife treatment system Multiplan v2.0.4 was also used to calculate the PDD for comparison with the results from GEANT4 and measurements.

B. GEANT4 simulation

GEANT4 is a simulation tool kit written in C++ language, which enables the simulation of propagation of particles that interact with the materials and/or other particles. It is widely used in many different scientific fields, such as high energy and nuclear physics [33], environment radiation detections [34], medical physics [29, 31, 35], and other applications [36, 37].

In this work, the simulations of the electromagnetic (EM) processes in GEANT4 have been performed with Low Energy package [38]. This Low Energy package includes the photoelectric effect, Compton scattering, Rayleigh scattering, gamma conversion, bremsstrahlung and ionization. Fluorescence of excited atoms is also considered. The current implementation of low energy processes is valid for energies down to 250 eV. Data used for the

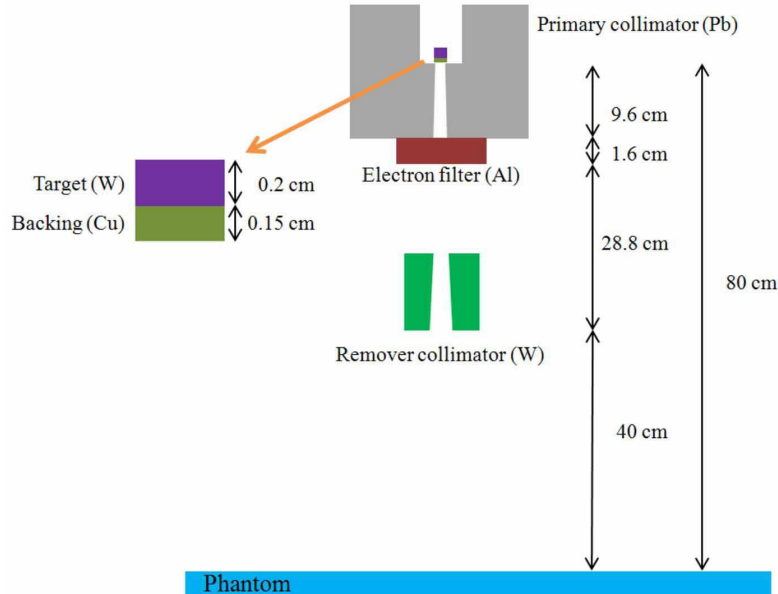


FIG. 2: (Color online) A schematic diagram of the CyberKnife system used in the simulations.

determination of cross sections and for sampling the final state are extracted from a set of publicly distributed evaluated data libraries, EADL (Evaluated Atomic Data Library) [39], EEDL (Evaluated Electrons Data Library) [40], EPDL97 (Evaluated Photons Data Library) [41], and stopping power data [42–45].

In our previous study [31], we modeled a CyberKnife system at the Seoul Uridul Hospital and simulated the photon beams produced by 6 MV CyberKnife using GEANT4 (version 9.2.p01). Figure 2 shows a schematic diagram of the CyberKnife system used in the simulations. To make the simulation more efficient, the calculation procedure was split into two steps. The CyberKnife produces electrons impinging on the tungsten target, which creates bremsstrahlung photons. In the first step, we scored the energy and momentum distribution of the photons for 5 to 60 mm cone sizes arriving at the surface of the water phantom of SSD of 80 cm. As the cone sizes vary, different energy and momentum distributions are obtained. In the second step, the photon beams were generated at the surface of the water phantom in the direction towards the phantom material by using the energy and angular distributions of the photons as scored in the first step. This two step method can save computation time greatly. PDD distributions, output factors and off axis ratios were also calculated in the second step. In Ref. [31], we found that our calculated values of these quantities in this two step method agreed with our measured values with errors less than 2%.

In this work, we used the same photon beam distribution as scored in Ref. [31]. We modeled inhomogeneous phantoms with and without the EBT2 film. An EBT2 film consists of 5 layers with different thickness and element compositions. Detailed information of the film used in our simulations is available from the product specification [46]. For the simulations with the EBT2 film, the size of the scoring voxel is chosen to have the thickness of the active layer of the EBT2 film which is $30 \mu\text{m}$. The lateral lengths of the voxels are set to 0.5, 1 and 3 mm for 5, 10 and 30 mm of cone sizes, respectively. The same conditions for the positions and sizes of the scoring voxels are used for the case of the simulations without the EBT2 film. First, we have performed benchmark simulations to confirm the consistency between our GEANT4 simulations and some previous studies [12, 22] done by others. Both homogeneous [12] and inhomogeneous [22] phantoms were considered. In this benchmark simulation also, we have considered phantoms with and without the EBT film included. In the simulations the production cut for the photons and the electrons was set to 10 keV and 100 keV, respectively. Each simulation was repeated ten times with different random number seeds. The results from these ten different simulations were averaged to get the final results and statistical errors. Simulation results are compared with our experimental results.

III. RESULTS AND DISCUSSION

A. Benchmark of our GEANT4 simulations with previous studies

In order to check the validity of our GEANT4 simulations, we have first calculated PDDs for homogeneous and inhomogeneous phantoms with conditions as given in Refs. [12] and [22]. As mentioned earlier, simulations have been performed in two cases; with and without the EBT film. First, the simulations are done with only polystyrene phantom without the EBT film. In this case, the absorbed doses were calculated in the polystyrene phantom. As noted in the Introduction, the calculated doses in this way are referred as DTP. Second, the simulations are done by taking into account the presence of the EBT film. The doses calculated in this way are referred to as DTF.

EBT films have different types and lot numbers. It was reported that the calculations of the absorbed dose have dependency on the type of EBT films if the energy of the photons is

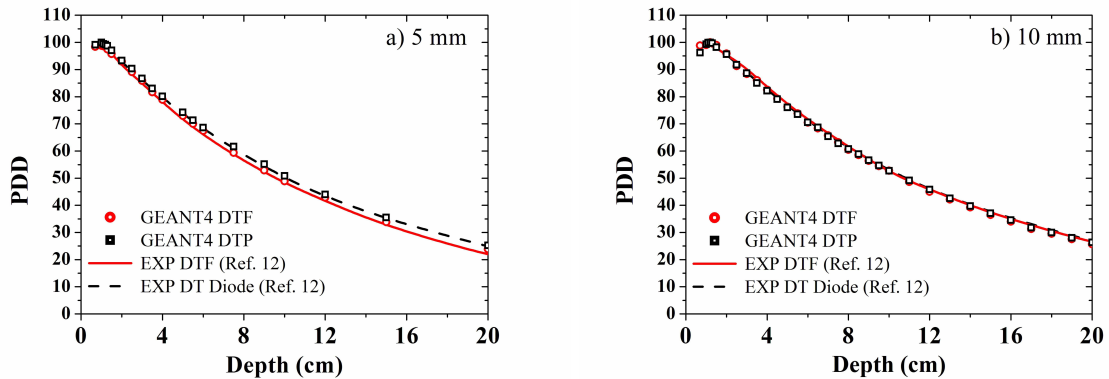


FIG. 3: (Color online) PDD distributions in water phantom for 5 and 10 mm cone sizes. The solid and the dashed lines represent the measured dose [12] values with film and diode detectors, respectively. The open circles and the open squares denote the calculated doses with and without the EBT film, respectively. DTF (DTP) refers to dose to film (dose to phantom). For a cone size of 10 mm the DTP and the DTF are the same, but for a small cone size of 5 mm the DTF is smaller than the DTP by about 5%. For both cases, our GEANT4 calculations agree with the measured values.

below 0.3 MeV [47]. To check the dependency of PDD calculations on the type of EBT films for the case of CyberKnife we used, we have considered three different types of EBT films: EBT1, EBT2 (lot020609) and EBT2 (lot031109), but discrepancies are not observed within the calculation errors of 0.5% for all the cases considered in this work. It may be because the photon beam energy from the 6MV CyberKnife is much higher than the photon beams used in Ref. [47]. Therefore, we shall not distinguish different types of the EBT films in this work and refer to the EBT2 film used in this work simply as the EBT film.

Let us first compare the PDD obtained from our simulations with the published PDD [12] in homogeneous water phantom. Figure 3 (b) shows good agreements between our calculations and the measurements obtained for 10 mm cone size regardless of the presence of the EBT film. The difference between the doses obtained from GEANT4 and the measured doses is smaller than 1.5% on the average for 10 mm cone size. Similar good agreements are observed for 30 mm cone size, though the comparison is not shown in Fig. 3. For 5 mm cone size, the doses obtained from GEANT4 with EBT film (without EBT film) still agree well with the measured doses with EBT film (with diode detector) with errors of 3.6% (1.7%), respectively. However, the PDD with EBT film is slightly smaller than that without the

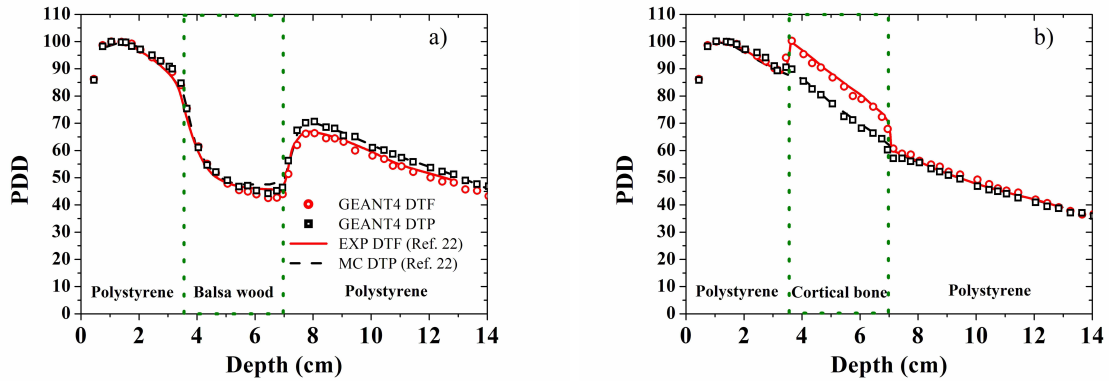


FIG. 4: (Color online) PDD distributions in an inhomogeneous phantom for a beam of 10 mm cone size. The solid and the dashed lines represent dose measured with EBT film and that calculated without the EBT film, respectively [22]. The open circles and the open squares denote our calculated doses with and without EBT film, respectively.

EBT film. The average ratio of the measured dose to diodes (DT diodes) to the measured DTF was 1.055. A similar value of 1.035 is obtained for the average ratio of the GEANT4 DTP to the GEANT4 DTF.

Second, we compare our calculated PDD with the calculated and measured PDD [22] for inhomogeneous phantoms. Figure 4 (a) and (b) show the PDD in inhomogeneous phantom with the Balsa wood and cortical bone, respectively. In the case when the Balsa wood is inserted in the phantom, our calculations reproduce well the PDD measured and calculated in Ref. [22]. Figure 4 (a) shows some difference between the doses with and without EBT films in our calculations as observed in the previous results [22] in the region beyond the Balsa wood. Also, Fig. 4 (b) shows that when cortical bone equivalent material is inserted in the phantom our calculations with and without EBT film reproduce the PDD measured with EBT film [22] and the PDD calculated without EBT film, respectively. Thus previous calculations and measurements [22] are well reproduced by our calculations, which confirms the accuracy of our GEANT4 calculations for both cases with and without the EBT film. This results also shows that the presence of the EBT film affects the value of PDD for a small cone size of 5 mm and needs to be properly taken into consideration in the simulation.

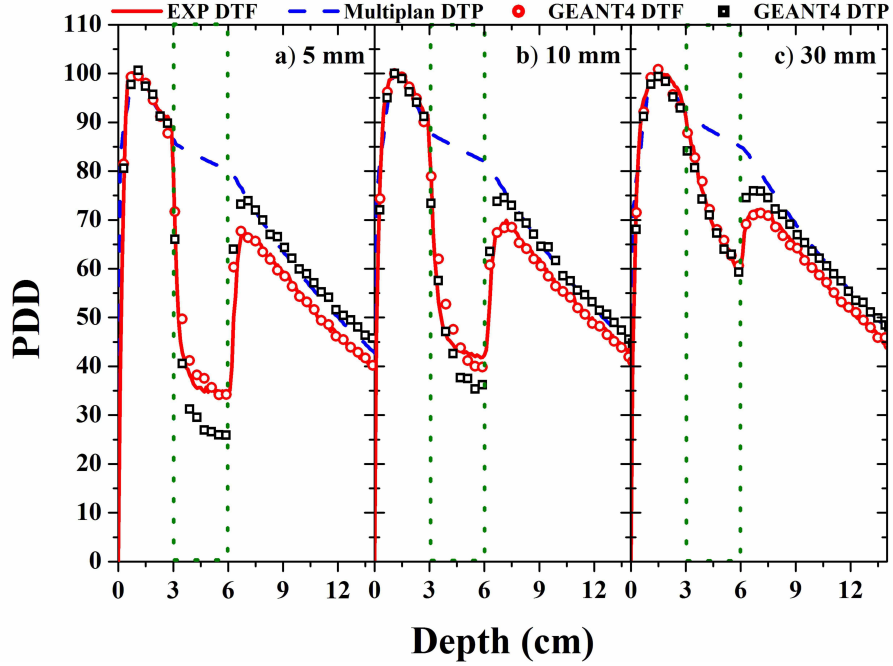


FIG. 5: (Color online) PDD distributions in an inhomogeneous phantom with Balsa wood for three field sizes (5, 10 and 30 mm). The solid line denotes the PDD measured with the EBT film. The dashed line represents the calculated dose values by using Multiplan. The open circles and the open squares denote the calculated PDD with and without the EBT film, respectively. GEANT4 DTF reproduces well EXP DTF.

B. Comparison of simulations with experiments with inhomogeneity of water-lung-water

We performed the calculations and measurements of PDDs for an inhomogeneous phantom with Balsa wood for three field sizes of 5, 10, 30 mm, and the results are represented in Fig. 5. The PDD calculated with the EBT film (GEANT4 DTF) reproduce well the PDD measured with the EBT film (EXP DTF). The average percentage errors between the GEANT4 DTF and the EXP DTF for 5, 10 and 30 mm of cone sizes are 2.20%, 0.43% and 0.08%, respectively. However, Multiplan cannot reproduce the measured dose values in both the Balsa wood region and beyond the Balsa wood region. Large discrepancies are observed especially in the Balsa wood region. The average ratio of the PDD obtained from Multiplan to those measured with EBT film for 5, 10 and 30 mm of field sizes are 2.1, 1.8 and 1.2, respectively, which shows larger discrepancies for smaller cone sizes. The same tendency can

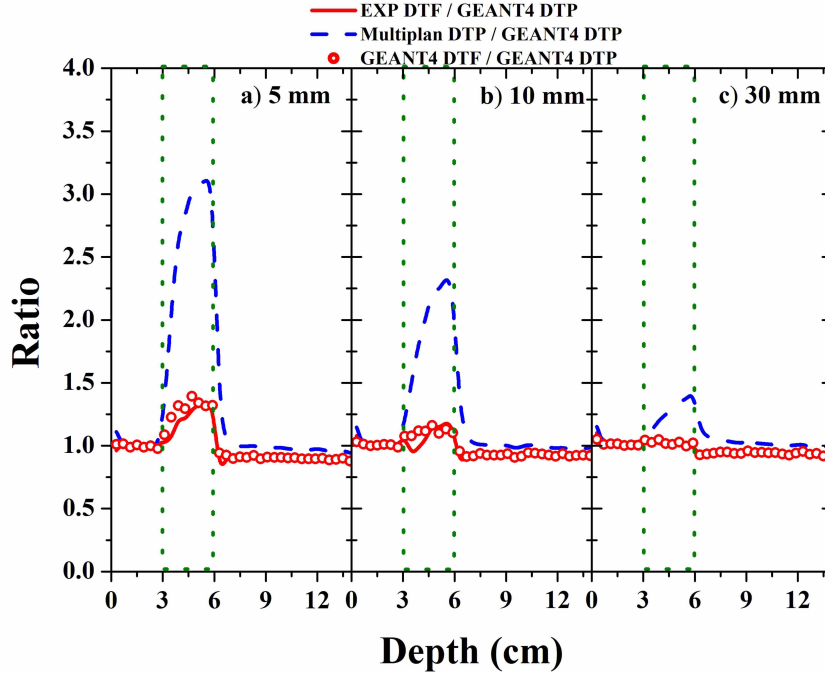


FIG. 6: (Color online) The ratios of the three different PDD's to the GEANT4 DTP are plotted as a function of the depth. The ratio of the measured DTF to GEANT4 DTP is shown by the solid line which agrees with that of the GEANT4 DTF to the GEANT4 DTP denoted by the open circles. The ratio of the DTP calculated from Multiplan to the calculated DTP is plotted by the dashed line.

also be seen in Ref. [22]. Figure 5 also shows there is a significant difference between the PDD calculated without the EBT film (GEANT4 DTP) and the PDD measured with the EBT film. This clearly shows that the proper inclusion of the EBT film in the simulation is necessary for accurate calculations of the dose. In Fig. 6 we have compared the GEANT4 DTP with the calculated and measured DTF. In the Balsa wood region, the average ratios of the EXP DTF to the GEANT4 DTP are 1.29, 1.11, and 1.02 for 5, 10 and 30 mm cone sizes, respectively. The average ratios of the DTP obtained from Multiplan to the GEANT4 DTP are 2.66, 1.95, and 1.26 for 5, 10, and 30 mm cone sizes, respectively. In the region beyond Balsa wood, the average ratios of the EXP DTF to the GEANT4 DTP are 0.90, 0.93, and 0.94 for 5, 10, and 30 mm cone sizes, respectively, whereas the average ratios of the DTP from Multiplan to the GEANT4 DTP are 0.99, 1.01, and 1.02, respectively, for 5, 10, and 30 mm cone sizes. When the EBT film is included, the doses in the Balsa wood region are enhanced and those in the region beyond Balsa wood are reduced. As the cone

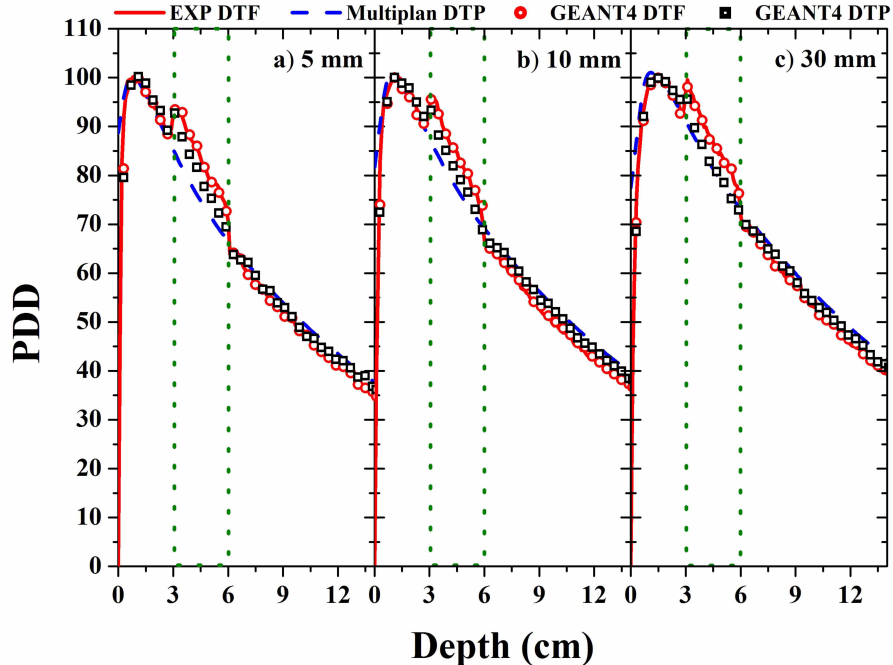


FIG. 7: (Color online) PDD distributions for the inhomogeneous phantom with soft bone material for three field sizes (5, 10 and 30 mm). The solid line denotes the experimental PDD measured with EBT film. The dashed line represents the PDD calculated with Multiplan. The open circles and open squares denote the doses calculated by GEANT4 with and without the EBT film, respectively. The open circles (GEANT4 DTF) and the experimental DTF agree with each other very well.

size increases, the discrepancy decreases, which shows that accurate estimates and measurements of doses are important particularly for small field sizes. Similar features are observed in Refs. [18], [21] and [22].

C. Comparison of simulations with experiments with inhomogeneity of water-bone-water

The PDDs for an inhomogeneous phantom with the soft bone are presented in Fig. 7. The average percentage errors between the GEANT4 DTF and the measured EXP DTF for 5, 10, 30 mm of cone sizes are 0.41%, 0.30% and 0.09%, respectively. On the other hand, Multiplan cannot reproduce the dose values in the soft bone regions. In contrast to the inhomogeneous phantom with Balsa wood, the discrepancies appear only in the soft bone region. Figure 8 shows the differences between the dose with the EBT film and that

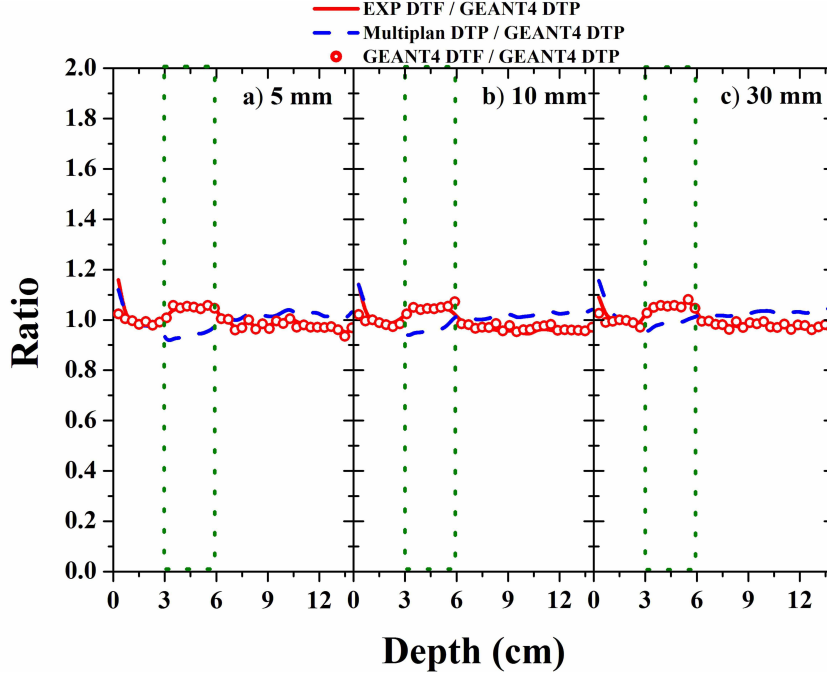


FIG. 8: (Color online) The ratios of the GEANT4 DTF and measured EXP DTF to the GEANT4 DTP are represented. The ratios of the calculated DTP obtained from Multiplan to the GEANT4 DTP are also shown.

without the EBT film. In the soft bone region, the average ratios of the GEANT4 DTF (and experimental DTF) to the GEANT4 DTP are 1.05, 1.05 and 1.05 for 5, 10 and 30 mm cone sizes, respectively. The average ratios of the DTP obtained from Multiplan to the GEANT4 DTP are 0.94, 0.96, and 0.99 for 5, 10, and 30 mm cone sizes, respectively. It can be seen that the ratios of the DTF to DTP are nearly constant as 1.05 and independent of the cone sizes.

Difference between the doses to water and the doses to other media was studied by Siebers *et al.* [23]. They suggested correction factors for various beam energies and materials. For the case of the 6MV photon beams, correction factors needed for the lung, ICRU tissue, soft bone and cortical bone are 1, 1.101, 1.035 and 1.117, respectively. Wilcox *et al.* [22] showed that the values of the DTP multiplied by the correction factor 1.117 in the cortical bone region agree with those of the doses obtained with the EBT film. From our study, the average ratios of DTF to DTP are obtained to be 1.049 ± 0.015 and 1.129 ± 0.015 for soft bone and cortical bone, respectively. Our ratios (1.049 and 1.129) and the correction factors (1.035 and 1.117) of Ref. [23] agree with each other within 1.3%.

IV. CONCLUSION

We have studied the PDD distributions in an inhomogeneous phantom with low and high density materials. Measurements were performed with Gafchromic EBT film using the 6MV CyberKnife system at the Seoul Uridul Hospital. The CyberKnife system was modeled and PDDs were calculated with GEANT4 code. Simulations have been performed with and without the EBT film. We find that it is important to include the presence of EBT film to accurately calculate the PDD values, in particular, for small field sizes. Comparison of the simulation results with the measured ones with EBT film shows that our calculations agree with the measurements within an error of 2.2% for all the cases considered here. However, Multiplan provided by the CyberKnife cannot reproduce the measured PDD. We confirm the correction factors suggested by Ref. [23] for the case when high density materials (soft bone or cortical bone) are inserted in the phantoms. The doses to phantom (DTP) without the EBT film can be different from the doses to film (DTF) by 29% for 5 mm cone size. Thus the presence of the EBT film needs to be taken into account in particular for small fields.

Acknowledgments

This work was supported by the National Research Foundation (NRF) of Korea grant funded by the Korean government (MEST) (No. 2012000486) and WCU program through NRF funded by the MEST (R31-2008-10029).

-
- [1] W. Lutz, K.R. Winston and N. Maleki, *Int. J. Radiat. Oncol. Biol. Phys.* **14**, 373 (1988).
 - [2] J.R. Adler, Jr., M.J. Murphy, S.D. Chang and S.L. Hancock, *Neurosurgery* **44**, 1299-1306; discussion 1306-1297 (1999).
 - [3] Elekta., "Elekta 1996 Leksell GammaPlan Instructions for Use for Version 4.0-Target Series (Geneva: Elekta)." (1996).
 - [4] A.L. Boyer, T.G. Ochransky, C.E. Nyerick, T.J. Waldron and C.J. Huntzinger, *Med. Phys.* **19**, (1992).
 - [5] J.M. Galvin, A.R. Smith and B. Lally, *Int. J. Radiat. Oncol. Biol. Phys.* **25**, 181 (1993).

- [6] E.B. Podgorsak, G.B. Pike, M. Pla, A. Olivier and L. Souhami, *Radiother. Oncol.* **17**, 349 (1990).
- [7] A.S. Saini and T.C. Zhu, *Med. Phys.* **31**, 914 (2004).
- [8] A.S. Saini and T.C. Zhu, *Med. Phys.* **34**, 1704 (2007).
- [9] P.W. Hoban, M. Heydariyan, W.A. Beckham and A.H. Beddoe, *Phys. Med. Biol.* **39**, 1219 (1994).
- [10] S.N. Rustgi and D.M. Frye, *Med. Phys.* **22**, 2117 (1995).
- [11] W.L. McLaughlin, C.G. Soares, J.A. Sayeg, E.C. McCullough, R.W. Kline and A. Wu, A.H. Maitz, *Med. Phys.* **21**, 379 (1994).
- [12] E.E. Wilcox and G.M. Daskalov, *Med. Phys.* **34**, 1967 (2007).
- [13] S.T. Chiu-Tsao, Y. Ho, R. Shankar, L. Wang and L.B. Harrison, *Med. Phys.* **32**, 3350 (2005).
- [14] S. Devic, J. Seuntjens, E. Sham, E.B. Podgorsak, C.R. Schmidlein, A.S. Kirov and C.G. Soares, *Med. Phys.* **32**, 2245 (2005).
- [15] C. Fiandra, U. Ricardi, R. Ragona, S. Anglesio, F.R. Giglioli, E. Calamia and F. Lucio, *Med. Phys.* **33**, 4314 (2006).
- [16] O.A. Zeidan, S.A. Stephenson, S.L. Meeks, T.H. Wagner, T.R. Willoughby, P.A. Kupelian and K.M. Langen, *Med. Phys.* **33**, 4064 (2006).
- [17] C. Martens, N. Reynaert, C. De Wagter, P. Nilsson, M. Coghe, H. Palmans, H. Thierens and W. De Neve, *Med. Phys.* **29**, 1528 (2002).
- [18] L. Paelinck, N. Reynaert, H. Thierens, W. De Neve and C. De Wagter, *Phys. Med. Biol.* **48**, 1895 (2003).
- [19] H. Saitoh, T. Fujisaki, R. Sakai and E. Kunieda, *Int. J. Radiat. Oncol. Biol. Phys.* **53**, 1380 (2002).
- [20] L. Wang, E. Yorke and C.S. Chui, *Int. J. Radiat. Oncol. Biol. Phys.* **50**, 1339 (2001).
- [21] L. Paelinck, N. Reynaert, H. Thierens, W. De Neve and C. De Wagter, *Phys. Med. Biol.* **50**, 2055 (2005).
- [22] E.E. Wilcox and G.M. Daskalov, *Med. Phys.* **35**, 2259 (2008).
- [23] J.V. Siebers, P.J. Keall, A.E. Nahum and R. Mohan, *Phys. Med. Biol.* **45**, 983 (2000).
- [24] S. Agostinelli *et al.*, *Nucl. Instrum. Methods Phys. Res., Sect. A* **506**, 250 (2003).
- [25] J.F. Carrier, L. Archambault, L. Beaulieu and R. Roy, *Med. Phys.* **31**, 484 (2004).
- [26] E. Poon, J. Seuntjens and F. Verhaegen, *Phys. Med. Biol.* **50**, 681 (2005).

- [27] E. Poon and F. Verhaegen, *Med. Phys.* **32**, 1696 (2005).
- [28] S. Elles, V.N. Ivanchenko, M. Maire and L. Urban, *Journal of Physics: Conference Series* **102**, 012009 (2008).
- [29] J.W. Shin, S.W. Hong, C.I. Lee and T.S. Suh, *J. Korean Phys. Soc.* **59**, 12 (2011).
- [30] A.L. McKenzie, *Br. J. Radiol. Suppl.* **25**, 46 (1996).
- [31] C.I. Lee, J.W. Shin, H.J. Shin, J.Y. Jung, Y.L. Kim, J.H. Min, S.W. Hong, S.M. Chung, W.G. Jung and T.S. Suh, *Korean J. Med. Phys.* **21**, 192 (2010).
- [32] D.R. White, R.J. Martin and R. Darlison, *Br. J. Radiol.* **50**, 814 (1977).
- [33] V.N. Ivanchenko, *Nucl. Instrum. Methods. Phys. Res. A.* **494**, 514 (2002).
- [34] P. M. Joshirao, J. W. Shin and *et al*, *Appl. Radiat. Isotopes* **81**, 184 (2013).
- [35] S.-B. Tang, Z.-J. Yin, H. Huang, Y. Cheng, F.-H. Cheng and F.-H. Mao, *Nucl. Sci. Tech.* **17**, 276 (2006).
- [36] J. W. Shin, T. S. Park, S. W. Hong, J. K. Park, J. T. Kim and J. S. Chai, *J. Korean Phys. Soc.* **59**, 2022 (2011).
- [37] S.I. Bak, T.S. Park, S.W. Hong, J.W. Shin and I.S. Hahn, *J. Korean Phys. Soc.* **59**, 2071 (2011).
- [38] Physics Reference Manual on the web <http://geant4.web.cern.ch/>.
- [39] S. T. Perkins, D. E. Cullen, M. H. Chen, J. H. Hubbell, J. Rathkopf and J. Scofield, Report UCRL-50400, Vol. **30**, 1991.
- [40] S. T. Perkins, D. E. Cullen and S. M. Seltzer, Report UCRL-50400 Vol. **31**, 1991.
- [41] D. E. Cullen, J. H. Hubbell and L. Kissel, Report UCRL-50400, Vol. **6**, Rev. 5, 1997.
- [42] H. H. Andersen and J. F. Ziegler, *Hydrogen: Stopping Powers and Ranges in All Elements. The Stopping and Ranges of Ions in Matter* (Pergamon, New York, 1977), Vol. 3.
- [43] J. F. Ziegler, *The Stopping and Ranges of Ions in Matter* (Pergamon, New York, 1977), Vol. 4.
- [44] J. F. Ziegler, J. P. Biersack and U. Littmark, *The Stopping and Range of Ions in Solids* (Pergamon, New York, 1985), Vol. 1.
- [45] ICRU, ICRU Report 49, 1993.
- [46] <http://online1.ispcorp.com/Gafchromic/content/products/ebt2/pdfs/EBT2productSpec.pdf>.
- [47] J.G. Sutherland and D.W. Rogers, *Med. Phys.* **37**, 1110 (2010).